

平成 26 年度 学位申請論文

論文題目

**Dietary salt restriction improves cardiac and adipose tissue pathology**

**independently of obesity in a rat model of metabolic syndrome**

(食塩摂取制限はメタボリック症候群ラットモデルにおいて、肥満とは無  
関係に心臓および脂肪組織の病態を改善する)

名古屋大学大学院医学系研究科

医療技術学専攻

(指導：永田 浩三 教授)

氏 名：服部 拓哉

## 要旨

**背景**—メタボリック症候群(MetS)は血圧の食塩感受性を高めるとともに心血管疾患の重要な危険因子である。MetSに関連した心筋傷害に及ぼす食塩制限の効果については不明な点が多い。

**方法および結果**—Dahl食塩感受性ラットとZuckerラットの交配に由来するMetSモデルであるDahlS.Z-*Lepr<sup>fa</sup>/Lepr<sup>fa</sup>* (DS/obese)ラットに生後9週齢より正食塩食(0.36% NaCl含)または低食塩食(0.0466% NaCl含)を投与し、生後15週齢において種々の解析を行った。ヘテロ同士の交配で生まれるDahlS.Z-*Lepr<sup>+</sup>/Lepr<sup>+</sup>* (DS/lean)ラットに同様の処置を施し比較した。正食塩食を投与したDS/obeseラットでは収縮期血圧は進行性に上昇し、9週齢以降15週齢までDS/leanラットに比べて高値を示し、さらに左室肥大・線維化、左室弛緩障害および拡張期スティフネスの増大も認められた。また、心筋の酸化ストレス、炎症、レニン・アンジオテンシン・アルドステロン系(RAAS)の遺伝子発現の増加もみられた。DS/obeseラットに対する食塩制限は、血圧上昇、左室肥大・線維化および左室拡張障害を軽減した。心筋の酸化ストレス、炎症、RAAS遺伝子発現の抑制はDS/obeseラットとDS/leanラットの両系統で認められた。加えて、食塩制限はDS/obeseラットの体重や脂肪重量および内臓脂肪細胞のサイズに影響しなかったが、内臓脂肪の炎症の増加とインスリンシグナルの低下を有意に抑制した。DS/obeseラットにおいて食塩制限は空腹時血糖値には影響しなかったが、空腹時血中インスリン濃度を低下させた。

**結論**—本MetSモデルにおいて食塩摂取制限は、肥満に影響することなく、高血圧、心筋傷害およびインスリン抵抗性を改善する。

## **Abstract**

**Background**—Metabolic syndrome (MetS) enhances salt sensitivity of blood pressure and is an important risk factor for cardiovascular disease. The effects of dietary salt restriction on cardiac pathology associated with MetS remain unclear.

**Methods and Results**—We investigated whether dietary salt restriction might ameliorate cardiac injury in DahlS.Z-*Lep<sup>fa</sup>/Lep<sup>fa</sup>* (DS/obese) rats, which are derived from a cross between Dahl salt-sensitive and Zucker rats and represent a model of MetS. DS/obese rats were fed a normal-salt (0.36% NaCl in chow) or low-salt (0.0466% NaCl in chow) diet from 9 weeks of age and were compared with similarly treated homozygous lean littermates (DahlS.Z-*Lep<sup>+</sup>/Lep<sup>+</sup>*, or DS/lean rats). DS/obese rats fed the normal-salt diet progressively developed hypertension and showed left ventricular hypertrophy, fibrosis, and diastolic dysfunction at 15 weeks. Dietary salt restriction attenuated all of these changes in DS/obese rats. The levels of cardiac oxidative stress and inflammation and the expression of cardiac renin-angiotensin-aldosterone system genes were increased in DS/obese rats fed the normal-salt diet, and dietary salt restriction down-regulated these parameters in both DS/obese and DS/lean rats. In addition, dietary salt restriction attenuated the increase in visceral adipose tissue inflammation and the decrease in insulin signaling apparent in DS/obese rats without reducing body weight or visceral adipocyte size. Dietary salt restriction did not alter fasting serum glucose levels but it markedly decreased the fasting serum insulin concentration in DS/obese rats.

**Conclusions**—Dietary salt restriction not only prevents hypertension and cardiac injury but also ameliorates insulin resistance, without reducing obesity, in this model of MetS.

## Introduction

Obesity is the central and causal component of metabolic syndrome (MetS), which is a growing medical problem in industrialized countries as a result of changes in lifestyle.<sup>1</sup>

Obesity is also associated with an increased incidence of hypertension and a consequent increase in cardiovascular disease risk.<sup>2</sup> Adipose tissue is thought to play an important role in the development of hypertension and complications related to insulin resistance as a result of dysregulated secretion of adipocytokines from adipocytes in visceral fat of obese humans.<sup>3</sup>

Hypertension is a key feature of MetS, and up to one-third of hypertensive individuals are thought to have MetS.<sup>4</sup> Excessive consumption of dietary salt is an important contributor to hypertension in humans.<sup>5</sup> A recent Chinese study showed that MetS enhances the blood pressure response to salt intake.<sup>6</sup> Indeed, dietary salt restriction reduced blood pressure to a greater extent in obese individuals than in nonobese ones.<sup>6,7</sup> In addition to its effects on blood pressure, high sodium intake elicits insulin resistance<sup>8</sup> and is thought to have detrimental cardiovascular effects independent of blood pressure.<sup>9</sup>

The INTERSALT study showed that a reduction in sodium intake resulted in a lowering of the prevalence of hypertension.<sup>10</sup> The Japanese Society of Hypertension Guidelines for the Management of Hypertension recommend a reduction in dietary salt intake to <6 g per day for the treatment of hypertension.<sup>11</sup> A reduced intake of dietary sodium is especially effective in lowering blood pressure in individuals with several risk factors for MetS.<sup>6</sup> In contrast, several surveys demonstrated an inverse association of cardiovascular mortality with salt intake.<sup>12-14</sup> The relation between cardiovascular mortality and salt intake is still controversial and the effects of dietary salt restriction on cardiac injury in individuals with MetS remain unclear.

We recently established a new animal model of MetS, the DahlS.Z-*Lep<sup>fa</sup>*/*Lep<sup>fa</sup>* (DS/obese) rat, by crossing Dahl salt-sensitive (DS) rats with Zucker rats harboring a

missense mutation in the leptin receptor gene (*Lepr*). When fed a normal diet, DS/obese rats develop a phenotype similar to MetS in humans, including hypertension and cardiac hypertrophy as well as renal and liver damage.<sup>15</sup> These observations suggested that salt sensitivity of blood pressure and target organ damage are enhanced in MetS. We have now investigated the effects of dietary salt restriction on cardiac and adipose tissue pathophysiology in male DS/obese rats.

## **Methods**

### **Animals and experimental protocols**

Animal experiments were approved by the Animal Experiment Committee of Nagoya University Graduate School of Medicine (Daiko district, approval Nos. 021-029, 022-009, 023-028, 024-012, 025-010, and 026-039). Eight-week-old male inbred DS/obese and DahlS.Z-*Lepr*<sup>+</sup>/*Lepr*<sup>+</sup> (DS/lean) rats were obtained from Japan SLC Inc. (Hamamatsu, Japan) and were handled in accordance with the guidelines of Nagoya University Graduate School of Medicine as well as with the Guide for the Care and Use of Laboratory Animals (NIH publication no. 85-23, revised 1996). After weaning, the rats were fed a 0.36% NaCl (normal-salt) diet. DS/obese rats were fed a normal-salt (NS) diet (0.36% NaCl in chow) or low-salt (LS) diet (0.0466% NaCl in chow) from 9 weeks of age and were compared with similarly treated homozygous lean littermates, DS/lean rats ( $n = 10, 10, 8,$  and  $8$  rats for DS/lean+LS, DS/lean+NS, DS/obese+LS, and DS/obese+NS groups, respectively). Both the normal-salt and low-salt diets and tap water were provided ad libitum throughout the experimental period. Body weight as well as food and water intake were measured weekly. At 15 weeks of age, the animals were anesthetized by intraperitoneal injection of ketamine (50 mg/kg) and xylazine (10 mg/kg) and were subjected to echocardiographic and hemodynamic analyses. The heart and both visceral (retroperitoneal) and subcutaneous (inguinal) fat were

subsequently excised, and left ventricular (LV) tissue was separated for analysis.

### **Echocardiographic and hemodynamic analyses**

Systolic blood pressure (SBP) was measured weekly in conscious animals by tail-cuff plethysmography (BP-98A; Softron, Tokyo, Japan). At 15 weeks of age, rats were subjected to transthoracic echocardiography, as described previously.<sup>16</sup> In brief, M-mode echocardiography was performed with a 12.5-MHz transducer (Xario SSA-660A; Toshiba Medical Systems, Tochigi, Japan). LV end-diastolic (LVDD) and end-systolic (LVDS) dimensions as well as the thickness of the interventricular septum (IVST) and LV posterior wall (LVPWT) were measured. LV fractional shortening (LVFS), relative wall thickness (RWT), and LV mass were calculated as follows:  $LVFS (\%) = [(LVDD - LVDS)/LVDD] \times 100$ ;  $RWT = (IVST + LVPWT)/LVDD$ ; and  $LV \text{ mass (g)} = \{[(IVST + LVDD + LVPWT)^3 - (LVDD)^3] \times 1.04\} \times 0.8 + 0.14$ .<sup>17</sup> For assessment of LV diastolic function, we calculated the ratio of early to late ventricular velocities ( $E/A$ ), and the isovolumic relaxation time (IRT) from the pulsed Doppler echocardiographic data. After echocardiography, cardiac catheterization was performed as described previously.<sup>16</sup> Tracings of LV pressure and the electrocardiogram were digitized to determine LV end-diastolic pressure (LVEDP). The time constant of isovolumic relaxation ( $\tau$ ) was calculated by the derivative method of Raff and Glantz as described previously.<sup>18</sup>

### **Measurement of metabolic parameters**

Serum levels of glucose, triglyceride, total cholesterol, and free fatty acid were measured by routine enzymatic assays. The concentration of insulin in serum was measured using a mouse/rat enzyme-linked immunosorbent assay kit (Morinaga Bioscience Institute, Yokohama, Japan). Insulin resistance was assessed from fasting insulin and glucose levels, using the previously validated homeostasis model assessment (HOMA-IR);  $HOMA-IR = \text{fasting glucose (mmol/L)} \times \text{fasting insulin}(\mu\text{U/mL})/22.5$ .<sup>19</sup> The serum concentration of

adiponectin was measured with the use of a mouse/rat enzyme-linked immunosorbent assay kit (Otsuka Pharmaceutical Co., Ltd., Tokyo, Japan). The plasma concentration of tumor necrosis factor (TNF)- $\alpha$  and interleukin (IL)-6 were measured with the use of mouse/rat enzyme-linked immunosorbent assay kits (R&D systems, Inc. Minneapolis, USA).

### **Histological analysis**

LV tissue was fixed in ice-cold 4% paraformaldehyde for 48 to 72 h, embedded in paraffin, and processed for histology as described.<sup>20</sup> Transverse sections (thickness, 3  $\mu$ m) of the left ventricle were stained either with hematoxylin-eosin for routine histological examination or with Azan-Mallory solution for evaluation of the extent of fibrosis. Image analysis was performed with NIH Scion Image software (Scion Corp., Frederick, MD, USA) in a blinded manner to the experimental status of the animals.

### **Immunohistochemical analysis**

For evaluation of macrophage infiltration into the LV myocardium or visceral fat, tissue sections were subjected to immunostaining with antibodies to the monocyte-macrophage marker CD68. Frozen sections (thickness, 5  $\mu$ m) of LV tissue were fixed with acetone, and the visceral fat pad was fixed in ice-cold 4% paraformaldehyde for 48 to 72 h, embedded in paraffin, and sectioned at a thickness of 5  $\mu$ m.<sup>20</sup> Endogenous peroxidase activity in all sections was blocked by their exposure to methanol containing 0.3% hydrogen peroxide. Sections were incubated at 4°C first overnight with mouse monoclonal antibodies to CD68 (1:100 dilution, clone ED1; Chemicon, Temecula, CA) and then for 30 min with Histofine Simple Stain Rat MAX PO (Nichirei Biosciences, Tokyo, Japan). Immune complexes were visualized with diaminobenzidine and hydrogen peroxide, and the sections were counterstained with hematoxylin. The number of immunoreactive myocardial interstitial macrophages was counted in five separate high-power fields of each section and is expressed as CD68-positive cells per square millimeter. The adipocyte cross-sectional area was

measured for 50 or more cells per animal, and macrophage infiltration in adipose tissue was quantified as the ratio of the number of nuclei of CD68-positive cells to the total number of nuclei in five different low-power fields of each section. Image analysis was performed with NIH Scion Image software (ImageJ) in a blinded manner to the experimental status of the animals.

### **Assay of superoxide production**

Nicotinamide adenine dinucleotide phosphate (NADPH)-dependent superoxide production by homogenates prepared from freshly frozen LV tissue was measured with an assay based on lucigenin-enhanced chemiluminescence as described previously.<sup>21</sup> The chemiluminescence signal was sampled every minute for 10 min with a microplate reader (WALLAC 1420 ARVO MX/Light; Perkin-Elmer, Waltham, MA), and the respective background counts were subtracted from experimental values. Sections stained with dihydroethidium (Sigma) were examined with a fluorescence microscope equipped with a 585-nm long-pass filter. As a negative control, sections were incubated with superoxide dismutase (300 U/mL) before staining with dihydroethidium; such treatment prevented the generation of fluorescence signals (data not shown). The average of dihydroethidium fluorescence intensity values was calculated with NIH ImageJ software.

### **Quantitative RT-PCR analysis**

Total RNA was extracted from LV tissue and treated with DNase with the use of a spin-vacuum isolation kit (Promega, Madison, WI). Total RNA was extracted from adipose tissue homogenized with QIAzol reagent with the use of an RNeasy Lipid Tissue Mini Kit for adipose tissue (Qiagen, Hilden, Germany). Complementary DNA was synthesized from 2  $\mu$ g (LV tissue) or 1  $\mu$ g (adipose tissue) of the total RNA by RT with the use of random primers (Invitrogen, Carlsbad, CA) and MuLV reverse transcriptase (Applied Biosystems, Foster City, CA). After reverse transcription (RT), real-time polymerase chain reaction (PCR) analysis



was performed with the use of a Prism 7000 Sequence Detector (Perkin-Elmer, Wellesley, MA)<sup>22</sup> and with primers and TaqMan probes specific for rat cDNAs encoding atrial natriuretic peptide (ANP),<sup>23</sup> brain natriuretic peptide (BNP),<sup>23</sup>  $\beta$ -myosin heavy chain ( $\beta$ -MHC),<sup>23</sup> collagen type I or type III,<sup>24</sup> fibronectin,<sup>25</sup> the p22<sup>phox</sup>,<sup>26</sup> gp91<sup>phox</sup>,<sup>26</sup> p47<sup>phox</sup>,<sup>27</sup> p67<sup>phox</sup>,<sup>27</sup> and Rac1<sup>27</sup> subunits of NADPH oxidase, monocyte chemoattractant protein (MCP)-1,<sup>28</sup> osteopontin,<sup>28</sup> cyclooxygenase (COX)-2,<sup>16</sup> angiotensin-converting enzyme (ACE),<sup>23</sup> the angiotensin II type 1A receptor (AT<sub>1A</sub>),<sup>23</sup> the mineralocorticoid receptor (MR),<sup>28</sup> serum- and glucocorticoid-regulated kinase (Sgk) 1,<sup>27</sup> TNF- $\alpha$ ,<sup>27</sup> or IL-6.<sup>27</sup> Reagents for detection of human 18S rRNA (Applied Biosystems) were used to quantify rat 18S rRNA as an internal standard.

### **Immunoblot analysis**

Total protein was isolated from LV and visceral adipose tissue and quantitated with the use of the Bradford reagent (Bio-Rad, Hercules, CA). Equal amounts of protein were subjected to SDS-polyacrylamide gel electrophoresis, and the separated proteins were transferred to a polyvinylidene difluoride membrane as described previously.<sup>16</sup> The membrane was incubated first with a 1:200 dilution of rabbit polyclonal antibodies to the MR (Santa Cruz Biotechnology, Santa Cruz, CA, USA) and a 1:1000 dilution of rabbit polyclonal antibodies to the Akt, Akt phosphorylated on Ser<sup>473</sup>, p70 S6 kinase, and p70 S6 kinase phosphorylated on Thr<sup>389</sup> (Cell Signaling Technology, Danvers, MA, USA) and then with a 1:10000 dilution of horseradish peroxidase-conjugated goat antibodies to rabbit immunoglobulin G (KPL Laboratories, Gaithersburg, MD, USA). Antibodies to GAPDH (Santa Cruz Biotechnology) were used to confirm equal loading of samples. Detection and quantification of immune complexes were performed as described previously.<sup>16</sup>

### **Statistical analysis**

Data are presented as means  $\pm$  SEM. Differences among groups of rats at 15 weeks of age

were assessed by one-way factorial analysis of variance (ANOVA) followed by Fisher's multiple-comparison test. The time courses of body weight, SBP, or food or water intake were compared among groups by two-way repeated-measures ANOVA [time course (8 to 15 weeks of age)  $\times$  salt loading (LS or NS)]. Furthermore, we analyzed the data using 2-way factorial ANOVA to evaluate the interactive influence of strains and salt loading on various parameters in the four experimental groups. A *P* value of  $<0.05$  was considered statistically significant.

## **Results**

### **Physiological analysis and metabolic parameters**

Body weight, visceral and subcutaneous fat mass, and the cross-sectional area of visceral adipocytes were markedly greater in DS/obese rats than in DS/lean rats (Figure 1A, Table 1). These parameters did not differ significantly, however, between animals of the same genotype fed a normal- or low-salt diet, indicating that dietary salt restriction had no effect on body or fat mass. Food and water intake were significantly greater in DS/obese rats than in DS/lean rats throughout the experimental period (Figure 1B, C; Table 1). Given that food intake did not differ between animals of the same genotype fed a normal- or low-salt diet, dietary salt intake in each type of rat fed a low-salt diet was approximately one-eighth of that in those fed a normal-salt diet. Dietary salt restriction significantly reduced water intake in DS/obese rats.

The metabolic parameters are summarized in Table 1. Dietary salt restriction did not alter fasting serum glucose levels but it markedly decreased the fasting serum insulin concentration and HOMA-IR index in DS/obese rats. In addition, dietary salt restriction significantly increased the serum levels of triglyceride and total cholesterol but it did not change the serum concentration of free fatty acid. Serum adiponectin levels were greater in DS/obese rats than in DS/lean rats and did not differ significantly between animals of the

same genotype fed a normal- or low-salt diet. Plasma levels of TNF- $\alpha$  and IL-6 were increased in DS/obese rats compared with DS/lean rats, and these effects were significantly attenuated by dietary salt restriction.

### **Hemodynamics, LV geometry, and cardiac function**

DS/obese rats fed a normal-salt diet progressively developed hypertension during the experimental period, and this change was significantly attenuated by dietary salt restriction (Figure 1D, Table 1). In contrast, DS/lean rats fed a normal- or low-salt diet maintained a normal SBP. At 15 weeks of age, the ratio of LV weight to tibial length, an index of LV hypertrophy, was increased in DS/obese rats compared with DS/lean rats, and this increase was significantly attenuated by dietary salt restriction (Table 1).

Echocardiography revealed that the thickness of the IVST and LVPWT, LVFS, RWT, and LV mass were significantly greater in DS/obese rats than in DS/lean rats, whereas the LVDD was similar in both rat strains (Table 2). Dietary salt restriction did not affect LVDD or LVFS, but it significantly attenuated the increases in IVST, LVPWT, RWT, and LV mass in DS/obese rats. IRT and tau, both of which are indices of LV relaxation, as well as the ratio of LVEDP to LVDD, an index of diastolic stiffness, were all increased in DS/obese rats compared with DS/lean rats. The  $E/A$  was decreased in DS/obese rats compared with DS/lean rats. Dietary salt restriction attenuated all of these changes in parameters of LV relaxation and diastolic stiffness in DS/obese rats.

### **Cardiomyocyte hypertrophy as well as cardiac fibrosis**

The cross-sectional area of cardiac myocytes was greater in DS/obese rats than in DS/lean rats, and this cardiomyocyte hypertrophy in DS/obese rats was significantly attenuated by dietary salt restriction (Figure 1E, F). Hemodynamic overload resulted in marked up-regulation of the expression of ANP, BNP, and  $\beta$ -MHC genes in the left ventricle of DS/obese rats, and this up-regulation was greatly attenuated by dietary salt restriction (Figure

1G–I).

Azan-Mallory staining revealed that fibrosis in perivascular and interstitial regions of the LV myocardium was increased in DS/obese rats compared with DS/lean rats and that this increase in myocardial fibrosis was significantly suppressed by dietary salt restriction (Figure 2A–C). The abundance of collagen type I and fibronectin mRNAs in the left ventricle as well as the ratio of the amount of collagen type I mRNA to that of collagen type III mRNA, which correlates with myocardial stiffness, were also increased in DS/obese rats in a manner sensitive to dietary salt restriction (Figure 2D–F).

### **Cardiac oxidative stress**

Superoxide production in myocardial tissue sections revealed by staining with dihydroethidium as well as the activity of NADPH oxidase in LV homogenates were both increased in DS/obese rats compared with DS/lean rats (Figure 2G–I). Dietary salt restriction significantly attenuated superoxide production and NADPH oxidase activity in both DS/obese and DS/lean rats. In particular, dietary salt restriction in DS/obese rats reduced these parameters to the levels apparent in DS/lean rats fed a normal-salt diet. The expression of genes for the p22<sup>phox</sup> and gp91<sup>phox</sup> membrane components and for the p47<sup>phox</sup>, p67<sup>phox</sup>, and Rac1 cytosolic components of NADPH oxidase in the left ventricle was also up-regulated in DS/obese rats compared with DS/lean rats (Figure 2J–N). Dietary salt restriction reduced the expression of these NADPH oxidase subunit genes in both DS/obese and DS/lean rats.

### **Cardiac inflammation**

Immunostaining of the LV myocardium for the monocyte-macrophage marker CD68 revealed that the number of CD68-positive cells was increased in DS/obese rats compared with DS/lean rats, and that dietary salt restriction reduced the extent of macrophage infiltration in both DS/lean and DS/obese rats (Figure 3A, B). The expression of MCP-1, osteopontin, and COX-2 genes in the left ventricle was also increased in DS/obese rats in a manner sensitive to

dietary salt restriction (Figure 3C–E). The expression of MCP-1 and osteopontin genes was also down-regulated by dietary salt restriction in DS/lean rats.

### **Cardiac renin-angiotensin-aldosterone system**

Cardiac expression of ACE, AT<sub>1A</sub>, MR, and Sgk1 genes was up-regulated in DS/obese rats compared with DS/lean rats, and dietary salt restriction down-regulated the expression of these genes in both DS/lean and DS/obese rats (Figure 3F–I). The abundance of the MR protein in the left ventricle showed a pattern similar to that of the MR mRNA in the 4 experimental groups (Figure 3J). In particular, dietary salt restriction in DS/obese rats down-regulated the expression of these genes of the renin-angiotensin-aldosterone system (RAAS) and that of MR protein to the levels apparent in DS/lean rats fed a normal-salt diet.

### **Inflammation in adipose tissue**

Immunostaining of visceral fat with antibodies to CD68 revealed the presence of more macrophages in DS/obese rats than in DS/lean rats (Figure 4A, B). DS/obese rats fed a normal-salt diet also exhibited more areas of aggregated CD68-positive cells surrounding adipocytes, forming a typical crownlike pattern, than did the other groups of animals. The increase in the extent of macrophage infiltration in adipose tissue of DS/obese rats was attenuated by dietary salt restriction. The expression of MCP-1, COX-2, TNF- $\alpha$ , and IL-6 genes in adipose tissue was also increased in DS/obese rats in a manner sensitive to dietary salt restriction (Figure 4C–F).

### **Insulin signaling in adipose tissue**

The ratio of the amount of the phospho-Ser<sup>473</sup> form of Akt to that of total Akt was significantly decreased in DS/obese rats compared with DS/lean rats, and this effect was restored to the level apparent in DS/lean rats by dietary salt restriction (Figure 4G). The phosphorylation of p70 S6 kinase on Thr<sup>389</sup> was significantly increased in DS/obese rats in a manner sensitive to dietary salt restriction (Figure 4H).

### **Analysis by 2-way factorial ANOVA**

There were no interactions between strains and salt loading in body weight, tibial length, food intake, or water intake (Table 3). The interactions were significant in SBP and LV weight, whereas it was not significant in heart rate. There were no interactions in adipose tissue weights or visceral adipocyte cross-sectional area. Although the interaction was not significant in glucose, they were significant in insulin and HOMA-IR. Regarding lipid metabolism, significant interactions were detected in triglyceride and total cholesterol, but it was not in free fatty acid. In regard to circulating adipocytokines, although there was no interaction in adiponectin, the interactions were significant in TNF- $\alpha$  and IL-6. With regard to echocardiographic and hemodynamic analyses, in IVST, LVPWT, RWT, LV mass, *E/A*, IRT, Tau, LVEDP, and LVEDP/LVDd, the interactions were all significant. Significant interactions were observed in myocyte cross-sectional area, perivascular and interstitial fibrosis, and the expression of fetal-type cardiac genes and profibrotic genes. There were no significant interactions in cardiac oxidative stress, the expression of NADPH oxidase components, inflammation (except for COX-2), or the expression of RAAS genes (except for MR protein). Finally, the interactions between both were all significant in adipose tissue analyses. Thus, the data analyzed by two-way factorial ANOVA were compatible with the original results analyzed by one-way factorial ANOVA.

### **Discussion**

We have shown that dietary salt restriction attenuated hypertension as well as LV hypertrophy, fibrosis, and diastolic dysfunction and that these effects were accompanied by inhibition of cardiac oxidative stress, inflammation, and RAAS gene expression in DS/obese rats. The antioxidative and anti-inflammatory effects of dietary salt restriction, without a lowering of blood pressure, were also apparent, in DS/lean rats. In addition, dietary salt restriction

inhibited inflammation in visceral adipose tissue without reducing body weight or visceral fat mass in DS/obese rats. Attenuation of insulin resistance induced by dietary salt restriction may have contributed to beneficial effects on cardiac pathophysiology, in a manner independent of its antihypertensive effect, in this model of MetS. However, dietary salt restriction was not beneficial in ameliorating dyslipidemia in DS/obese rats.

Our recent report suggested that the presence of the *fa* allele of *Lepr* on the DahlS background is associated with increased salt sensitivity of blood pressure.<sup>15</sup> In the present study, dietary salt restriction substantially attenuated the increase in blood pressure in DS/obese rats without affecting SBP in DS/lean rats. Insulin resistance, a key component of MetS, is also closely related to salt sensitivity of blood pressure.<sup>8</sup> Reduced systemic insulin resistance resulting from dietary salt restriction may thus have contributed to the attenuation of hypertension by this manipulation in DS/obese rats in the present study. However, the mechanism by which salt intake affects cardiovascular function remains uncertain. Our results suggest that dietary salt restriction may alter LV structure and function as well as blood pressure in hypertensive obese individuals but not in normotensive nonobese controls. In the present study, the beneficial effects of dietary salt restriction on LV remodeling and diastolic dysfunction could not be separated from the antihypertensive effect. Nevertheless, the pleiotropic benefits of dietary salt restriction may help explain the relations between salt intake and cardiovascular and all-cause mortality.<sup>29</sup>

The cardiac inflammatory changes may have contributed to myocardial fibrosis in DS/obese rats.<sup>30</sup> Dietary salt restriction attenuated macrophage infiltration into the myocardium as well as the up-regulation of MCP-1, osteopontin, and COX-2 gene expression in the heart of DS/obese rats, indicating that dietary salt restriction alleviated cardiac inflammation in these animals. Moreover, the increase in circulating levels of TNF- $\alpha$  and IL-6 in DS/obese rats was inhibited by dietary salt restriction. Since the elevations in

circulating proinflammatory cytokines also result in cardiac fibrosis and dysfunction,<sup>31, 32</sup> the decrease in these cytokines by dietary salt restriction may have contributed to improvement of cardiac injury in DS/obese rats. Given that dietary salt restriction significantly attenuated cardiac inflammation and slightly but not significantly down-regulated the expression of profibrotic genes without lowering blood pressure in DS/lean rats, salt loading appears to contribute to the development of cardiac inflammation and consequent up-regulation of profibrotic genes in a manner independent of blood pressure. In this regard, however, dietary salt restriction did not affect cardiac fibrosis in DS/lean rats under our experimental conditions.

The decrease in cardiac oxidative stress induced by dietary salt restriction in both DS/obese and DS/lean rats was accompanied by a reduction in blood pressure only in DS/obese rats. Salt loading may be an important trigger for the accumulation of reactive oxygen species in MetS, which in turn may play a key role in salt-induced progression of cardiac pathophysiology associated with this condition.<sup>33</sup> Our observations that the cardiac RAAS was inhibited by dietary salt restriction in both DS/obese and DS/lean rats are consistent with previous results showing that high salt intake increases aldosterone production and up-regulates  $AT_{1A}$  mRNA in the cardiovascular system of rats.<sup>34</sup> Enhanced MR signaling in the myocardium results in increased cardiac oxidative stress and inflammation, leading to the development of cardiac remodeling and dysfunction.<sup>28, 33</sup> Although dietary salt restriction did not affect cardiac phenotype in DS/lean rats, our results suggest that the inhibition of cardiac oxidative stress and the cardiac RAAS induced by dietary salt restriction in DS/obese rats are not likely attributable solely to the reduction in blood pressure.

Visceral obesity gives rise to a state of chronic, low-grade inflammation that contributes to cardiovascular disease.<sup>35</sup> The low-grade inflammation in adipose tissue



associated with obesity is characterized by abnormal levels of circulating proinflammatory factors and an aberrant production of adipocytokines.<sup>35</sup> Indeed, we detected adipocyte hypertrophy, macrophage infiltration, and up-regulation of the expression of proinflammatory genes in visceral adipose tissue of DS/obese rats, consistent with previous studies showing macrophage infiltration into adipose tissue of obese animals<sup>36</sup> as well as obesity-induced inflammation and insulin resistance.<sup>37</sup> Dietary salt restriction did not affect adipocyte size but attenuated macrophage infiltration and the increased expression of proinflammatory genes in visceral adipose tissue of DS/obese rats. It did not affect any of these parameters in DS/lean rats. These data suggest that salt can modulate adipose tissue inflammation, but not adipose tissue mass, in MetS, and that macrophage accumulation in adipose tissue is a feature of MetS rather than obesity.

Previous studies have reported that severe dietary salt restriction elicits insulin resistance<sup>38</sup> and has caused adverse effects on glucose<sup>39</sup> and lipid metabolism.<sup>40</sup> Our data on lipid metabolism are consistent with a previous report showing that in obese mice, dyslipidemia induced by dietary salt restriction is attributable to an impairment in the removal rate of triglyceride-rich lipoproteins.<sup>40</sup> Moreover, our results are in good agreement with another report showing that free fatty acid levels did not vary on a low-salt diet.<sup>41</sup> Contrary to the previous report,<sup>40</sup> we observed that in DS/obese rats, dietary salt restriction ameliorated systemic insulin resistance, as shown by the reductions in the fasting insulin concentration and HOMA-IR index, in spite of increased triglyceride and total cholesterol concentrations. Because dietary salt restriction did not affect circulating adiponectin levels, adiponectin may not have played a major role in improvement of insulin resistance in this model of MetS. The phosphorylation of Akt clearly modulates the glucose transport and lipogenesis in the adipose tissue.<sup>8,38</sup> The p70 S6 kinase has been reported to inhibit insulin receptor substrate (IRS)-1 function through induction of serine phosphorylation of IRS-1,

which is believed to be the major mechanism of insulin resistance.<sup>42</sup> Moreover, TNF- $\alpha$  induces insulin resistance by increasing Ser/Thr phosphorylation of IRS-1.<sup>43</sup> Taken together, the present results suggest that p70 S6 kinase and consequent inhibition of the IRS-1/Akt pathway in adipose tissue contributed to insulin resistance in DS/obese rats, and that attenuation of p70 S6 kinase phosphorylation by dietary salt restriction improved the IRS-1/Akt kinase-mediated insulin signaling. Since insulin resistance is induced by inflammatory adipocytokines and excess salt via Rac1 activation,<sup>44</sup> suppression of Rac1 activation by dietary salt restriction might have contributed, at least in part, to improved insulin resistance. Thus, dietary salt restriction may have inhibited systemic and adipose tissue inflammation as well as improved insulin signaling in adipose tissue in DS/obese rats, resulting in a decrease in insulin levels.

In conclusion, dietary salt restriction ameliorated hypertension and cardiac pathophysiology in DS/obese rats. In addition, it did not alter adipose tissue mass but attenuated adipose tissue inflammation and improved insulin signaling in DS/obese rats. Dietary salt restriction in patients with MetS may be an effective strategy not only for preventing hypertension and cardiac injury but also for providing attenuation of insulin resistance, without reducing obesity.

### **Acknowledgments**

We thank Chieko Nakashima and Masafumi Ohtake for technical assistance.

### **Source of Funding**

This work was supported by unrestricted research grants from Nippon Boehringer Ingelheim Co., Ltd. (Tokyo, Japan), Ajinomoto Pharmaceuticals Co., Ltd. (Tokyo, Japan), Kyowa Hakko Kirin Co. Ltd. (Tokyo, Japan), Astellas Pharma Inc. (Tokyo, Japan), Mochida

Pharmaceutical Co., Ltd. (Tokyo, Japan), Mitsubishi Tanabe Pharma Corporation (Osaka, Japan), Takeda Pharmaceutical Company Limited (Osaka, Japan), Daiichi-Sankyo Company, Limited (Tokyo, Japan) and Dr. Nagata (Nagoya University) as well as by Management Expenses Grants from the Japanese government to Nagoya University.

### **Conflict of Interest/Disclosure**

None.

### **References:**

1. Grundy SM, Brewer HB, Jr., Cleeman JI, Smith SC, Jr., Lenfant C. Definition of metabolic syndrome: Report of the National Heart, Lung, and Blood Institute/American Heart Association conference on scientific issues related to definition. *Circulation*. 2004;109:433-438.
2. Lakka HM, Laaksonen DE, Lakka TA, Niskanen LK, Kumpusalo E, Tuomilehto J, Salonen JT. The metabolic syndrome and total and cardiovascular disease mortality in middle-aged men. *JAMA*. 2002;288:2709-2716.
3. Matsuzawa Y. Therapy Insight: adipocytokines in metabolic syndrome and related cardiovascular disease. *Nat Clin Pract Cardiovasc Med*. 2006;3:35-42.
4. Cuspidi C, Meani S, Fusi V, Severgnini B, Valerio C, Catini E, Leonetti G, Magrini F, Zanchetti A. Metabolic syndrome and target organ damage in untreated essential hypertensives. *J Hypertens*. 2004;22:1991-1998.
5. He FJ, MacGregor GA. A comprehensive review on salt and health and current experience of worldwide salt reduction programmes. *J Hum Hypertens*. 2009;23:363-384.
6. Chen J, Gu D, Huang J, Rao DC, Jaquish CE, Hixson JE, Chen CS, Chen J, Lu F, Hu D, Rice T, Kelly TN, Hamm LL, Whelton PK, He J. Metabolic syndrome and salt sensitivity of

- blood pressure in non-diabetic people in China: a dietary intervention study. *Lancet*. 2009;373:829-835.
7. Rocchini AP, Key J, Bondie D, Chico R, Moorehead C, Katch V, Martin M. The effect of weight loss on the sensitivity of blood pressure to sodium in obese adolescents. *N Engl J Med*. 1989;321:580-585.
8. Ogihara T, Asano T, Ando K, Sakoda H, Anai M, Shojima N, Ono H, Onishi Y, Fujishiro M, Abe M, Fukushima Y, Kikuchi M, Fujita T. High-salt diet enhances insulin signaling and induces insulin resistance in Dahl salt-sensitive rats. *Hypertension*. 2002;40:83-89.
9. Dyer AR, Elliott P, Shipley M, Stamler R, Stamler J. Body mass index and associations of sodium and potassium with blood pressure in INTERSALT. *Hypertension*. 1994;23:729-736.
10. Intersalt Cooperative Research Group. Intersalt: an international study of electrolyte excretion and blood pressure. Results for 24 hour urinary sodium and potassium excretion. *BMJ*. 1988;297:319-328.
11. Shimamoto K, Ando K, Fujita T, Hasebe N, Higaki J, Horiuchi M, Imai Y, Imaizumi T, Ishimitsu T, Ito M, Ito S, Itoh H, Iwao H, Kai H, Kario K, Kashihara N, Kawano Y, Kim-Mitsuyama S, Kimura G, Kohara K, Komuro I, Kumagai H, Matsuura H, Miura K, Morishita R, Naruse M, Node K, Ohya Y, Rakugi H, Saito I, Saitoh S, Shimada K, Shimosawa T, Suzuki H, Tamura K, Tanahashi N, Tsuchihashi T, Uchiyama M, Ueda S, Umemura S. The Japanese Society of Hypertension Guidelines for the Management of Hypertension (JSH 2014). *Hypertens Res*. 2014;37:253-387.
12. Stolarz-Skrzypek K, Kuznetsova T, Thijs L, Tikhonoff V, Seidlerova J, Richart T, Jin Y, Olszanecka A, Malyutina S, Casiglia E, Filipovsky J, Kawecka-Jaszcz K, Nikitin Y, Staessen JA. Fatal and nonfatal outcomes, incidence of hypertension, and blood pressure changes in relation to urinary sodium excretion. *JAMA*. 2011;305:1777-1785.
13. Alderman MH, Cohen H, Madhavan S. Dietary sodium intake and mortality: the National

- Health and Nutrition Examination Survey (NHANES I). *Lancet*. 1998;351:781-785.
14. Cohen HW, Hailpern SM, Fang J, Alderman MH. Sodium intake and mortality in the NHANES II follow-up study. *Am J Med*. 2006;119:275 e277-214.
15. Hattori T, Murase T, Ohtake M, Inoue T, Tsukamoto H, Takatsu M, Kato Y, Hashimoto K, Murohara T, Nagata K. Characterization of a new animal model of metabolic syndrome: the DahlS.Z-*Lepr<sup>fa</sup>/Lepr<sup>fa</sup>* rat. *Nutr Diabetes*. 2011;1:e1.
16. Murase T, Hattori T, Ohtake M, Nakashima C, Takatsu M, Murohara T, Nagata K. Effects of estrogen on cardiovascular injury in ovariectomized female DahlS.Z-*Lepr<sup>fa</sup>/Lepr<sup>fa</sup>* rats as a new animal model of metabolic syndrome. *Hypertension*. 2012;59:694-704.
17. Reffelmann T, Kloner RA. Transthoracic echocardiography in rats. Evaluation of commonly used indices of left ventricular dimensions, contractile performance, and hypertrophy in a genetic model of hypertrophic heart failure (SHHF-Mcc-facp-Rats) in comparison with Wistar rats during aging. *Basic Res Cardiol*. 2003;98:275-284.
18. Nagata K, Iwase M, Sobue T, Yokota M. Differential effects of dobutamine and a phosphodiesterase inhibitor on early diastolic filling in patients with congestive heart failure. *J Am Coll Cardiol*. 1995;25:295-304.
19. Matthews DR, Hosker JP, Rudenski AS, Naylor BA, Treacher DF, Turner RC. Homeostasis model assessment: insulin resistance and beta-cell function from fasting plasma glucose and insulin concentrations in man. *Diabetologia*. 1985;28:412-419.
20. Miyachi M, Yazawa H, Furukawa M, Tsuboi K, Ohtake M, Nishizawa T, Hashimoto K, Yokoi T, Kojima T, Murate T, Yokota M, Murohara T, Koike Y, Nagata K. Exercise training alters left ventricular geometry and attenuates heart failure in dahl salt-sensitive hypertensive rats. *Hypertension*. 2009;53:701-707.
21. Ichihara S, Noda A, Nagata K, Obata K, Xu J, Ichihara G, Oikawa S, Kawanishi S, Yamada Y, Yokota M. Pravastatin increases survival and suppresses an increase in myocardial

matrix metalloproteinase activity in a rat model of heart failure. *Cardiovasc Res*.

2006;69:726-735.

22. Somura F, Izawa H, Iwase M, Takeichi Y, Ishiki R, Nishizawa T, Noda A, Nagata K, Yamada Y, Yokota M. Reduced myocardial sarcoplasmic reticulum Ca(2+)-ATPase mRNA expression and biphasic force-frequency relations in patients with hypertrophic cardiomyopathy. *Circulation*. 2001;104:658-663.

23. Nagata K, Somura F, Obata K, Odashima M, Izawa H, Ichihara S, Nagasaka T, Iwase M, Yamada Y, Nakashima N, Yokota M. AT1 receptor blockade reduces cardiac calcineurin activity in hypertensive rats. *Hypertension*. 2002;40:168-174.

24. Sakata Y, Yamamoto K, Mano T, Nishikawa N, Yoshida J, Hori M, Miwa T, Masuyama T. Activation of matrix metalloproteinases precedes left ventricular remodeling in hypertensive heart failure rats: its inhibition as a primary effect of Angiotensin-converting enzyme inhibitor. *Circulation*. 2004;109:2143-2149.

25. Hattori T, Murase T, Sugiura Y, Nagasawa K, Takahashi K, Ohtake M, Miyachi M, Murohara T, Nagata K. Effects of salt status and blockade of mineralocorticoid receptors on aldosterone-induced cardiac injury. *Hypertens Res*. 2014;37:125-133.

26. Takatsu M, Nakashima C, Takahashi K, Murase T, Hattori T, Ito H, Murohara T, Nagata K. Calorie restriction attenuates cardiac remodeling and diastolic dysfunction in a rat model of metabolic syndrome. *Hypertension*. 2013;62:957-965.

27. Murase T, Hattori T, Ohtake M, Abe M, Amakusa Y, Takatsu M, Murohara T, Nagata K. Cardiac remodeling and diastolic dysfunction in DahlS.Z-*Lep<sup>fa</sup>/Lep<sup>fa</sup>* rats: a new animal model of metabolic syndrome. *Hypertens Res*. 2012;35:186-193.

28. Nagata K, Obata K, Xu J, Ichihara S, Noda A, Kimata H, Kato T, Izawa H, Murohara T, Yokota M. Mineralocorticoid receptor antagonism attenuates cardiac hypertrophy and failure in low-aldosterone hypertensive rats. *Hypertension*. 2006;47:656-664.

29. Cook NR, Cutler JA, Obarzanek E, Buring JE, Rexrode KM, Kumanyika SK, Appel LJ, Whelton PK. Long term effects of dietary sodium reduction on cardiovascular disease outcomes: observational follow-up of the trials of hypertension prevention (TOHP). *BMJ*. 2007;334:885-888.
30. Weber KT. From inflammation to fibrosis: a stiff stretch of highway. *Hypertension*. 2004;43:716-719.
31. Bradham WS, Bozkurt B, Gunasinghe H, Mann D, Spinale FG. Tumor necrosis factor-alpha and myocardial remodeling in progression of heart failure: a current perspective. *Cardiovasc Res*. 2002;53:822-830.
32. Melendez GC, McLarty JL, Levick SP, Du Y, Janicki JS, Brower GL. Interleukin 6 mediates myocardial fibrosis, concentric hypertrophy, and diastolic dysfunction in rats. *Hypertension*. 2010;56:225-231.
33. Matsui H, Ando K, Kawarazaki H, Nagae A, Fujita M, Shimosawa T, Nagase M, Fujita T. Salt excess causes left ventricular diastolic dysfunction in rats with metabolic disorder. *Hypertension*. 2008;52:287-294.
34. Schmid C, Castrop H, Reitbauer J, Della Bruna R, Kurtz A. Dietary salt intake modulates angiotensin II type 1 receptor gene expression. *Hypertension*. 1997;29:923-929.
35. Yudkin JS, Stehouwer CD, Emeis JJ, Coppack SW. C-reactive protein in healthy subjects: associations with obesity, insulin resistance, and endothelial dysfunction: a potential role for cytokines originating from adipose tissue? *Arterioscler Thromb Vasc Biol*. 1999;19:972-978.
36. Baudrand R, Lian CG, Lian BQ, Ricchiuti V, Yao TM, Li J, Williams GH, Adler GK. Long-term dietary sodium restriction increases adiponectin expression and ameliorates the proinflammatory adipokine profile in obesity. *Nutr Metab Cardiovasc Dis*. 2014;24:34-41.
37. Kamei N, Tobe K, Suzuki R, Ohsugi M, Watanabe T, Kubota N, Ohtsuka-Kawatari N, Kumagai K, Sakamoto K, Kobayashi M, Yamauchi T, Ueki K, Oishi Y, Nishimura S, Manabe

- I, Hashimoto H, Ohnishi Y, Ogata H, Tokuyama K, Tsunoda M, Ide T, Murakami K, Nagai R, Kadowaki T. Overexpression of monocyte chemoattractant protein-1 in adipose tissues causes macrophage recruitment and insulin resistance. *J Biol Chem.* 2006;281:26602-26614.
38. Prada PO, Coelho MS, Zecchin HG, Dolnikoff MS, Gasparetti AL, Furukawa LN, Saad MJ, Heimann JC. Low salt intake modulates insulin signaling, JNK activity and IRS-1<sup>ser307</sup> phosphorylation in rat tissues. *J Endocrinol.* 2005;185:429-437.
39. Prada P, Okamoto MM, Furukawa LN, Machado UF, Heimann JC, Dolnikoff MS. High- or low-salt diet from weaning to adulthood: effect on insulin sensitivity in Wistar rats. *Hypertension.* 2000;35:424-429.
40. Catanozi S, Rocha JC, Nakandakare ER, Passarelli M, Mesquita CH, Silva AA, Dolnikoff MS, Harada LM, Quintao EC, Heimann JC. The rise of the plasma lipid concentration elicited by dietary sodium chloride restriction in Wistar rats is due to an impairment of the plasma triacylglycerol removal rate. *Atherosclerosis.* 2001;158:81-86.
41. Townsend RR, Kapoor S, McFadden CB. Salt intake and insulin sensitivity in healthy human volunteers. *Clin Sci (Lond).* 2007;113:141-148.
42. Haruta T, Uno T, Kawahara J, Takano A, Egawa K, Sharma PM, Olefsky JM, Kobayashi M. A rapamycin-sensitive pathway down-regulates insulin signaling via phosphorylation and proteasomal degradation of insulin receptor substrate-1. *Mol Endocrinol.* 2000;14:783-794.
43. Ueno M, Carvalheira JB, Tambascia RC, Bezerra RM, Amaral ME, Carneiro EM, Folli F, Franchini KG, Saad MJ. Regulation of insulin signalling by hyperinsulinaemia: role of IRS-1/2 serine phosphorylation and the mTOR/p70 S6K pathway. *Diabetologia.* 2005;48:506-518.
44. Fujita T. Mineralocorticoid receptors, salt-sensitive hypertension, and metabolic syndrome. *Hypertension.* 2010;55:813-818.



## Figure Legends

**Figure 1.** Time course of body weight (**A**), food intake (**B**), water intake (**C**), and SBP (**D**) and effects of salt restriction on cardiomyocyte hypertrophy (**E–I**). (**E**) Hematoxylin-eosin staining of transverse sections of the LV myocardium. Scale bars, 50  $\mu\text{m}$ . (**F**) Cross-sectional area of cardiac myocytes determined from sections similar to those in (**A**). (**G–I**) Quantitative RT-PCR analysis of ANP, BNP, and  $\beta$ -MHC mRNAs, respectively. The amount of each mRNA was normalized by that of 18S rRNA and then expressed relative to the corresponding mean value for DS/lean rats fed a normal-salt diet. Data in (**A–D**) and (**F–I**) are means  $\pm$  SEM ( $n = 10, 10, 8,$  and  $8$  rats for DS/lean+LS, DS/lean+NS, DS/obese+LS, and DS/obese+NS groups, respectively). \* $P < 0.05$  versus DS/lean+LS; † $P < 0.05$  versus DS/lean+NS; ‡ $P < 0.05$  versus DS/obese+LS.

**Figure 2.** Effects of salt restriction on cardiac fibrosis and oxidative stress. (**A**) Representative microscopic images of collagen deposition (blue color) in perivascular (upper panels) or interstitial (lower panels) regions of the LV myocardium as revealed by Azan-Mallory staining. Scale bars, 50  $\mu\text{m}$  (upper panels) or 100  $\mu\text{m}$  (lower panels). (**B, C**) Relative extents of perivascular and interstitial fibrosis, respectively, in the LV myocardium as determined from sections similar to those in (**A**). (**D–F**) Quantitative RT-PCR analysis of collagen type I (**D**) and fibronectin (**F**) mRNAs as well as the ratio of the amount of collagen type I mRNA to that of collagen type III mRNA (**E**). (**G**) Representative microscopic images of superoxide production in the LV myocardium as revealed by staining with dihydroethidium. Scale bars, 100  $\mu\text{m}$ . (**H**) Dihydroethidium fluorescence intensity as determined from sections similar to those in (**G**) and expressed relative to the value for DS/lean rats fed a normal-salt diet. (**I**) NADPH-dependent superoxide production in LV homogenates. Data are expressed as relative light units (RLU) per milligram of protein.

(J–N) Quantitative RT-PCR analysis of p22<sup>phox</sup>, gp91<sup>phox</sup>, p47<sup>phox</sup>, p67<sup>phox</sup>, and Rac1 mRNAs, respectively. Data in (B–F) and (H–N) are means  $\pm$  SEM (*n* values and symbols for statistical significance are as in Figure 1).

**Figure 3.** Effects of salt restriction on cardiac inflammation and RAAS genes. (A) Representative microscopic images of immunohistochemical staining (brown) for the monocyte-macrophage marker CD68. Scale bars, 50  $\mu$ m. (B) Density of CD68-positive cells in the LV myocardium as determined from sections similar to those in (A). (C–I) Quantitative RT-PCR analysis of MCP-1, osteopontin, COX-2, ACE, AT<sub>1A</sub>, MR, and Sgk1 mRNAs, respectively. (J) Immunoblot analysis of the abundance of MR protein in the left ventricle. A representative immunoblot and the ratio of the amount of the MR to that of GAPDH (expressed relative to the corresponding value for the DS/lean+NS group) are shown. Data in (F–J) are means  $\pm$  SEM (*n* values and symbols for statistical significance are as in Figure 1).

**Figure 4.** Effects of salt restriction on adipose tissue inflammation and insulin signaling. (A) Representative microscopic images of immunohistochemical staining for CD68. Scale bars, 100  $\mu$ m. (B) The number of nuclei of CD68-positive cells as a percentage of total nuclei was determined from sections similar to those in (A). (C–F) Quantitative RT-PCR analysis of MCP-1, COX-2, and TNF- $\alpha$ , and IL-6 mRNAs, respectively. (G, H) Representative immunoblots and the ratio of phosphorylated (p-) to total forms of Akt and p70 S6 kinase. Data in (B–H) are means  $\pm$  SEM (*n* values and symbols for statistical significance are as in Figure 1).

**Table 1.** Physiological and metabolic parameters in rats of the four experimental groups at 15 weeks of age.

Parameter	DS/lean		DS/obese	
	LS	NS	LS	NS
Tibial length (mm)	39.0 ± 0.2	39.1 ± 0.2	35.9 ± 0.3*†	35.6 ± 0.3*†
Heart rate (beats/min)	370 ± 10	382 ± 8	350 ± 10†	368 ± 19
Heart weight/tibial length (mg/mm)	29.8 ± 0.6	30.5 ± 0.8	35.1 ± 1.2*†	40.3 ± 0.9*†‡
LV weight/tibial length (mg/mm)	21.5 ± 0.3	22.1 ± 0.5	26.1 ± 0.9*†	31.4 ± 0.6*†‡
Visceral fat weight/tibial length (mg/mm)	92.7 ± 6.2	98.3 ± 6.8	426.4 ± 12.6*†	431.6 ± 26.6*†
Subcutaneous fat weight/tibial length (mg/mm)	62.8 ± 5.5	63.3 ± 6.5	642.4 ± 23.7*†	612.3 ± 63.9*†
Visceral adipocyte cross-sectional area (µm <sup>2</sup> )	3380 ± 131	3467 ± 190	10544 ± 136*†	10698 ± 300*†
Glucose (mg/dL)	130.1 ± 4.3	131.8 ± 4.5	148.0 ± 18.9	147.0 ± 14.3
Insulin (ng/mL)	0.55 ± 0.17	0.38 ± 0.08	4.43 ± 1.14*†	7.17 ± 1.35*†‡
HOMA-IR	4.37 ± 1.26	3.05 ± 0.64	36.08 ± 8.01*†	72.39 ± 9.11*†‡
Triglyceride (mg/dL)	68.4 ± 5.8	65.5 ± 6.6	3469.3 ± 869.2*†	1304.9 ± 250.4*†‡
Total cholesterol (mg/dL)	73.6 ± 2.99	84.8 ± 4.47	469.25 ± 85.66*†	297.38 ± 22.73*†‡
Free fatty acid (mEq/L)	0.89 ± 0.09	0.95 ± 0.13	1.40 ± 0.11*†	1.54 ± 0.19*†
Adiponectin (ng/mL)	3965 ± 128	3729 ± 229	6257 ± 229*†	6030 ± 332*†
TNF-α (pg/mL)	4.21 ± 1.40	5.21 ± 0.90	6.33 ± 1.00*†	17.71 ± 3.13*†‡
IL-6 (pg/mL)	37.18 ± 8.30	35.88 ± 5.00	53.88 ± 9.60*†	122.01 ± 14.54*†‡

Analytes were measured in serum unless indicated otherwise. Data are means  $\pm$  SEM ( $n = 10$ , 10, 8, and 8 rats for DS/lean+LS, DS/lean+NS, DS/obese+LS, and DS/obese+NS groups, respectively). \* $P < 0.05$  versus DS/lean+LS; † $P < 0.05$  versus DS/lean+NS; ‡ $P < 0.05$  versus DS/obese+LS.

**Table 2.** Cardiac morphological and functional parameters of rats in the four experimental groups at 15 weeks of age.

Parameter	DS/lean		DS/obese	
	LS	NS	LS	NS
IVST (mm)	1.47 ± 0.04	1.51 ± 0.02	1.83 ± 0.03*†	2.08 ± 0.03*†‡
LVPWT (mm)	1.44 ± 0.04	1.49 ± 0.02	1.78 ± 0.04*†	2.06 ± 0.03*†‡
LVDd (mm)	8.09 ± 0.19	8.36 ± 0.19	8.60 ± 0.32	8.51 ± 0.22
LVFS (%)	37.7 ± 1.2	36.0 ± 0.9	44.4 ± 2.1*†	45.7 ± 1.9*†
RWT	0.36 ± 0.02	0.36 ± 0.01	0.43 ± 0.02*†	0.49 ± 0.02*†‡
LV mass (mg)	834 ± 30	920 ± 40	1290 ± 40*†	1528 ± 37*†‡
<i>E/A</i>	2.01 ± 0.05	2.01 ± 0.08	1.65 ± 0.09*†	1.34 ± 0.06*†‡
IRT (ms)	17.1 ± 0.6	17.8 ± 0.4	26.3 ± 1.0*†	31.5 ± 0.9*†‡
Tau (ms)	21.0 ± 1.1	23.0 ± 1.7	30.0 ± 0.5*†	39.8 ± 2.5*†‡
LVEDP (mmHg)	2.62 ± 0.36	2.50 ± 0.20	5.07 ± 0.48*†	8.27 ± 0.80*†‡
LVEDP/LVDd (mmHg/mm)	0.29 ± 0.02	0.28 ± 0.01	0.51 ± 0.03*†	0.85 ± 0.01*†‡

Data are means ± SEM ( $n = 10, 10, 8,$  and  $8$  rats for DS/lean+LS, DS/lean+NS, DS/obese+LS, and DS/obese+NS groups, respectively). \* $P < 0.05$  versus DS/lean+LS; † $P < 0.05$  versus DS/lean+NS; ‡ $P < 0.05$  versus DS/obese+LS.

**Table 3.** Results of two-way factorial ANOVA in four groups of rats (DS/lean+LS, DS/lean+NS, DS/obese+LS, and DS/obese+NS).

Variable	P value for the interaction	Variable	P value for the interaction
Body weight (g)	0.4098	ANP	<0.0001
Tibial length (mm)	0.3453	BNP	0.0002
Food intake (g/day)	0.5898	$\beta$ -MHC	0.0004
Water intake (mL/day)	0.0905	Perivascular fibrosis	0.0474
SBP (mmHg)	0.004	Interstitial fibrosis (%)	0.0006
Heart rate (beats/min)	0.7671	Collagen type I	0.0398
Heart weight/tibial length (mg/mm)	0.0122	Collagen type I/ collagen type III	0.0285
LV weight/tibial length (mg/mm)	0.0005	Fibronectin	0.0217
Visceral fat weight/tibial length (mg/mm)	0.9890	DHE staining	0.0762
Subcutaneous fat weight/tibial length (mg/mm)	0.6207	NADPH oxidase activity (RLU/mg protein)	0.060
Visceral adipocyte cross-sectional area ( $\mu\text{m}^2$ )	0.8717	p22 <sup>phox</sup>	0.8784
Glucose (mg/dL)	0.8876	gp91 <sup>phox</sup>	0.4404
Insulin (ng/mL)	0.0140	p47 <sup>phox</sup>	0.3057
HOMA-IR	0.0006	p67 <sup>phox</sup>	0.5990
Triglyceride (mg/dL)	0.0112	Rac1	0.0708

---

Total cholesterol (mg/dL)	0.0268	CD68 positive cells (/mm <sup>2</sup> )	0.0597
Free fatty acid (mEq/L)	0.7467	MCP-1	0.5691
Adiponectin (ng/mL)	0.9871	Osteopontin	0.0550
TNF- $\alpha$ (pg/mL)	0.0028	COX-2	0.0241
IL-6 (pg/mL)	0.0038	ACE	0.0905
IVST (mm)	0.0033	AT <sub>1A</sub>	0.8853
LVPWT (mm)	0.0015	MR	0.2082
LVDd (mm)	0.4473	Sgk1	0.1095
LVFS (mm)	0.3097	MR protein	<0.0001
RWT	0.0333	CD68 positive cells in adipose tissue (%)	0.0002
LV mass (mg)	0.0284	MCP-1 in adipose tissue	0.0105
<i>E/A</i>	0.0356	COX-2 in adipose tissue	0.0205
IRT (ms)	0.0023	TNF- $\alpha$ in adipose tissue	0.0215
Tau (ms)	0.0222	IL-6 in adipose tissue	0.0455
LVEDP (mmHg)	0.0043	Akt phosphorylation	0.0359
LVEDP/LVDd (mmHg/mm)	0.0088	p70S6K phosphorylation	0.0080
Myocyte cross-sectional area ( $\mu\text{m}^2$ )	<0.0001		

---

# Figure 1

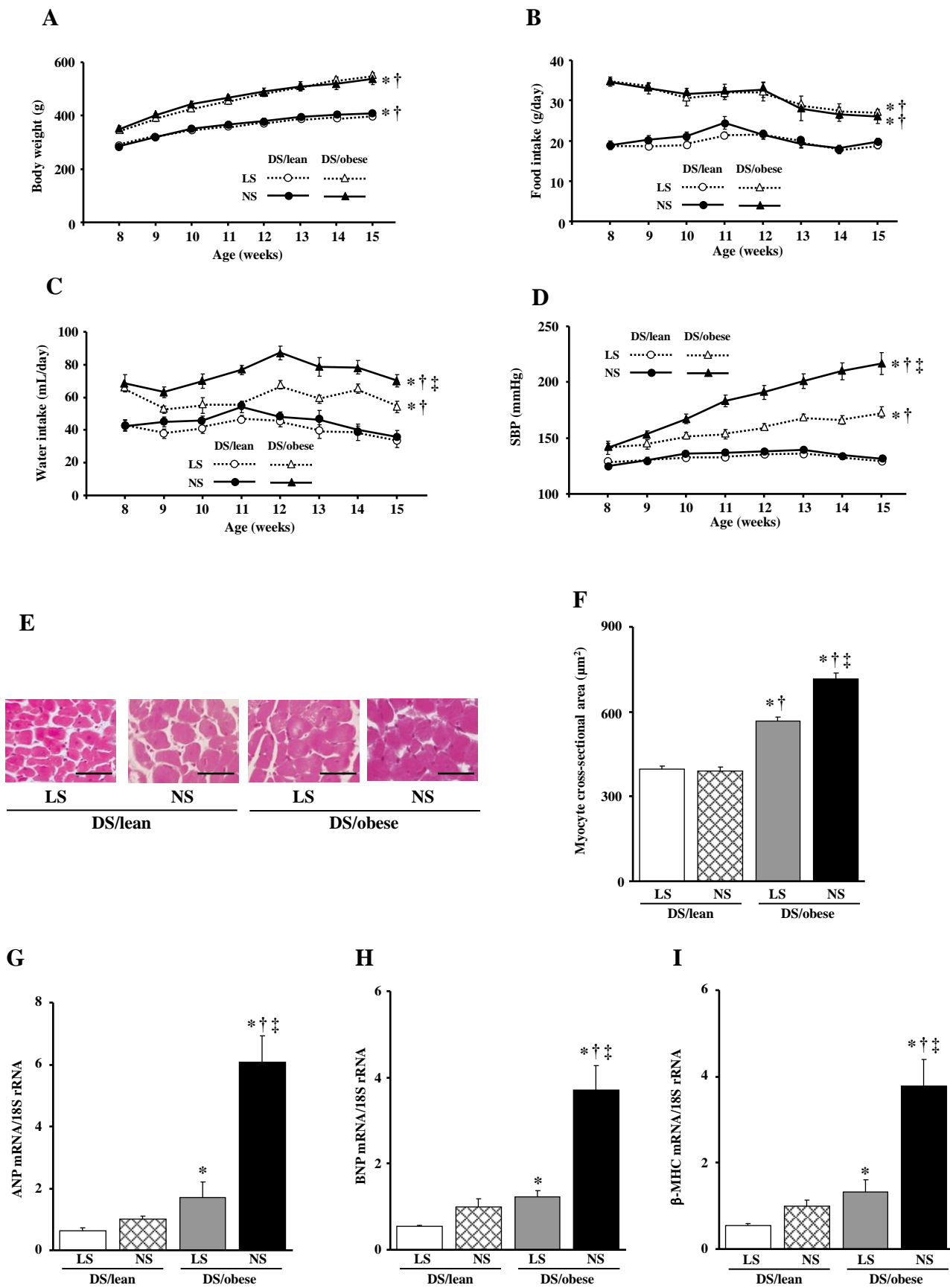
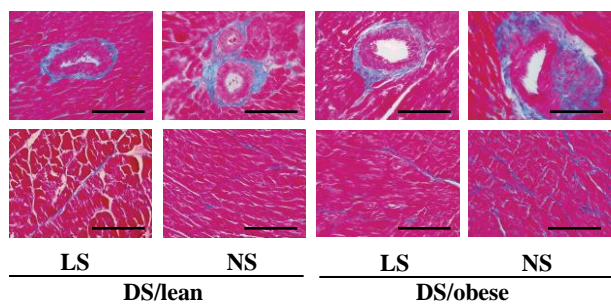


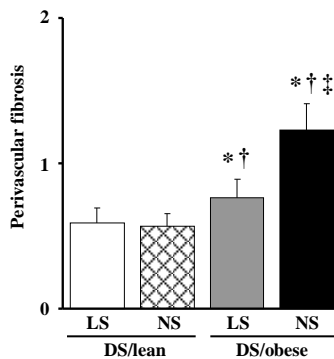


# Figure 2

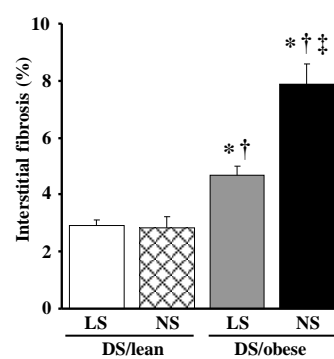
**A**



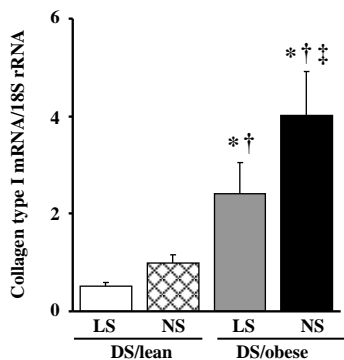
**B**



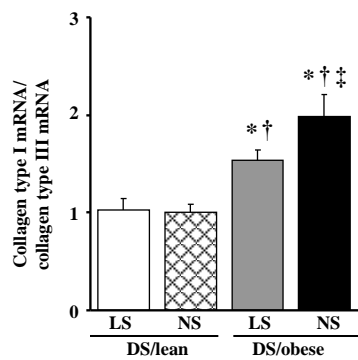
**C**



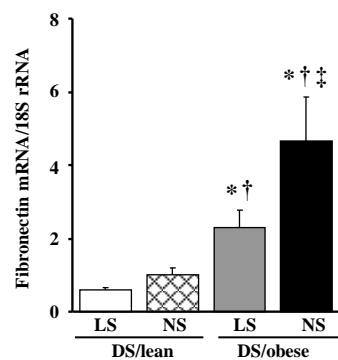
**D**



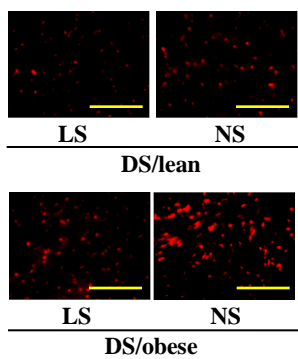
**E**



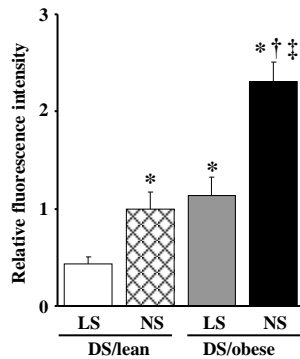
**F**



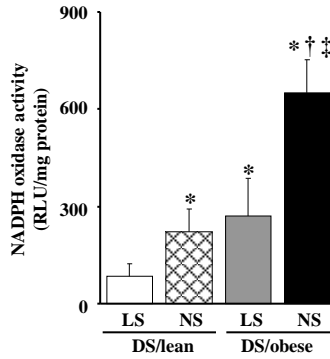
**G**



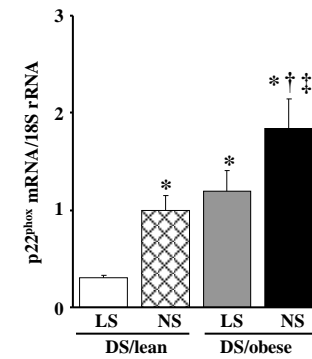
**H**



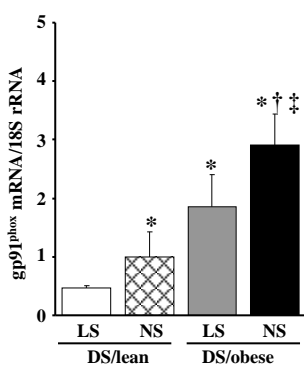
**I**



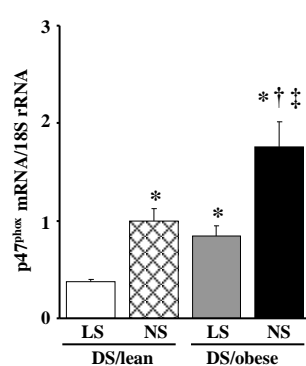
**J**



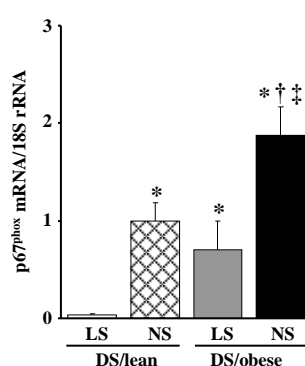
**K**



**L**



**M**



**N**

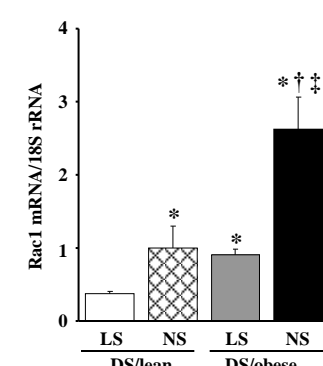


**Figure 3**

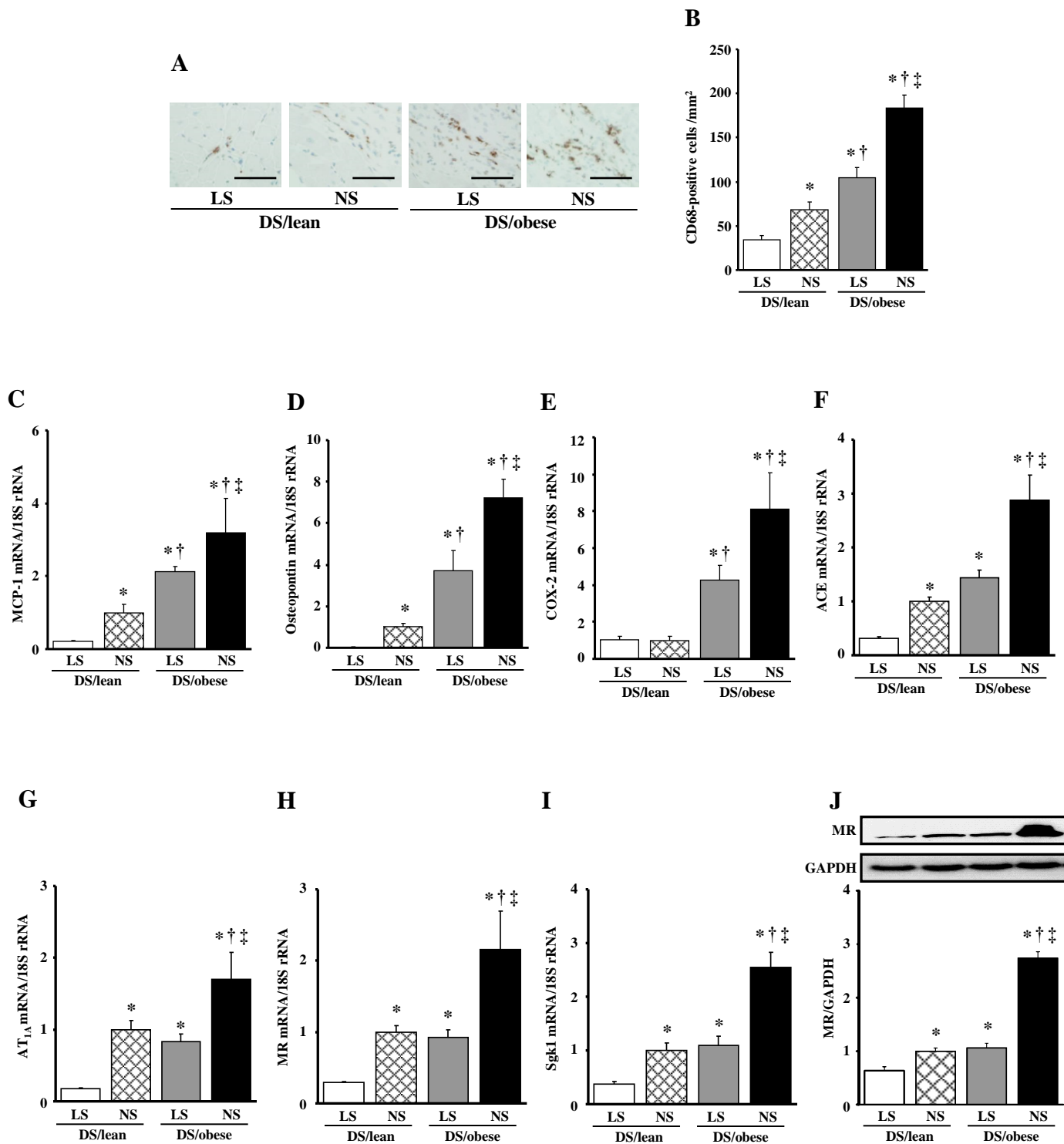


# Figure 4

